

X-TRACK: Physics-Aware xLSTM for Realistic Vehicle Trajectory Prediction

Aanchal Rajesh Chugh

Technische Hochschule Augsburg

TTZ Landsberg am Lech

Augsburg, Germany

aanchal.rajesh.chugh@tha.de

Marion Neumeier

Technische Hochschule Ingolstadt

Almotion

Ingolstadt, Germany

marion.neumeier@thi.de

Sebastian Dorn

Technische Hochschule Augsburg

TTZ Landsberg am Lech

Augsburg, Germany

sebastian.dorn@tha.de

Abstract—Recent advancements in Recurrent Neural Network (RNN) architectures, particularly the Extended Long Short Term Memory (xLSTM), have addressed the limitations of traditional Long Short Term Memory (LSTM) networks by introducing exponential gating and enhanced memory structures. These improvements make xLSTM suitable for time-series prediction tasks as they exhibit the ability to model long-term temporal dependencies better than LSTMs. Despite their potential, these xLSTM-based models remain largely unexplored in the context of vehicle trajectory prediction. Therefore, this paper introduces a novel xLSTM-based vehicle trajectory prediction framework, X-TRAJ, and its physics-aware variant, X-TRACK (eXtended LSTM for TRAjectory prediction Constraint by Kinematics), which explicitly integrates vehicle motion kinematics into the model learning process. By introducing physical constraints, the proposed model generates realistic and feasible trajectories. A comprehensive evaluation on the highD and NGSIM datasets demonstrates that X-TRACK outperforms state-of-the-art baselines.

Index Terms—xLSTM, vehicle trajectory prediction, physics-based kinematic layer

I. INTRODUCTION

In the domain of autonomous driving, one of the key challenges is to anticipate the future trajectories of the neighboring vehicles to plan its own trajectory [1], [2]. Vehicle motion is influenced not only by individual dynamics but also by social interactions and contextual dependencies among neighboring vehicles. Since the driving environment is highly dynamic, autonomous vehicles must precisely detect and anticipate the trajectories of surrounding vehicles, particularly during maneuvers such as lane changes, merging, or braking. Therefore, capturing social interactions and environmental context is crucial for accurate and reliable trajectory prediction. Additionally, to ensure the safety of traffic participants, such as neighboring cars, pedestrians, bikers, etc., the generated trajectories must be socially compliant and physically feasible.

Due to the ability of Recurrent Neural Networks (RNNs) to model temporal sequences, they are widely adopted in the field of vehicle trajectory prediction. Particularly, Long Short Term Memory (LSTM) [3] is used as an encoder and decoder for capturing temporal interactions in combination with modeling social interactions [4]–[6]. While RNNs, especially LSTMs, have been predominantly adopted in this field, these models often fail to ensure that predicted trajectories are physically

feasible or in accordance with the physical laws of vehicular motion. Therefore, a kinematic bicycle model was introduced where the predictions of a deep learning model are refined through a kinematic layer [7]. It incorporates the physical characteristics of the target vehicle, such as non-holonomic dynamics, to generate predictions consistent with real-world behavior. Integrating a physics-based layer, therefore, improves trajectory smoothness and feasibility.

However, conventional LSTMs exhibit several inherent limitations, including the inability to revise storage decisions, the compression of all information into a scalar-valued cell state, and a lack of parallelization due to sequential processing of data. To address these limitations, Beck et al. [8] introduced Extended Long Short Term Memory (xLSTM), an enhanced variant with improved memory dynamics, representational capacity, and computational efficiency. The extended family of LSTM now consists of sLSTM and mLSTM, where sLSTM has a scalar memory, a scalar update, and memory mixing, and mLSTM has matrix memory and a covariance update rule.

As evidenced in recent papers [9]–[12], xLSTM excels in time-series forecasting across a wide range of application areas. Although xLSTM has demonstrated strong performance in capturing long-range dependencies, its potential in the field of vehicle trajectory prediction remains underexplored. xLSTM offers architectural improvements that allow for richer memory representations than LSTMs and enhanced temporal abstraction, which are particularly beneficial for understanding vehicle interactions over extended time frames and forecasting the future motion of the target vehicle. Our work leverages the strengths of xLSTM as an encoder to present a novel trajectory prediction architecture, X-TRAJ.

To generate more realistic and physically consistent trajectories, the proposed framework integrates a physics-based kinematic model into the xLSTM-based trajectory prediction architecture. While learning-based models achieve high prediction accuracy by effectively recognizing motion patterns from data, they often disregard the physical laws governing vehicle dynamics and sometimes result in trajectories that are statistically plausible but physically infeasible, such as abrupt turns or unrealistically rapid accelerations [7]. In contrast, purely physics-based models strictly adhere to kinematic laws but often lack the flexibility to represent the complex, context-

dependent behavior observed in real traffic [13]. Explicitly incorporating vehicle dynamics into the data-driven learning process, the proposed hybrid models, termed X-TRACK (eXtended LSTM for TRAjectory prediction Constraint by Kinematics), leverage the strengths of both paradigms, generating trajectories that are not only accurate but also physically consistent with real-world vehicular motion.

The main contributions are as follows:

- A novel trajectory prediction framework that leverages xLSTMs' ability to model long-range temporal dependencies for predicting trajectories on highways.
- Investigation of the benefits and drawbacks of using sLSTM and mLSTM for encoding and decoding purposes with respect to the trajectory prediction task.
- Integration of a physics-based kinematic layer into an xLSTM-based prediction framework to predict trajectories in accordance with the vehicle dynamics.
- Performance evaluation on publicly available highD and NGSIM datasets.

II. RELATED WORK

Vehicle trajectory prediction is a research field that aims to accurately predict the motion of the target vehicle while minimizing residual errors over time horizons. There are two major challenges faced in trajectory prediction. First, difficulty in modeling social interactions between vehicles, such as avoiding a collision, following others, or moving in a group, significantly impacts the trajectory of the vehicle. Second, the trajectories of vehicles are highly non-deterministic, as with the same historical trajectory, there could be multiple feasible future paths converging to a single destination. The problem of trajectory prediction has been addressed using a wide range of approaches, from conventional rule-based methods to modern deep learning techniques. Conventional methods involve maneuver-based, physics-based, and interaction-aware motion models [14]–[16]. This section reviews existing deep learning-based models and physics-based approaches for vehicle trajectory prediction. For a comprehensive overview of the field, readers are referred to works of Lefèvre et al. [17] and Yin et al. [18].

A. Deep Learning-Based Trajectory Prediction

Due to the sequential structure of the trajectory prediction tasks, RNNs form the basis of most deep learning models. To model temporal dependencies in vehicular motion, RNNs such as LSTMs [3] and Gated Recurrent Units (GRUs) have been widely adopted. Alahi et al. [19] introduced Social LSTM, which employs pooling mechanisms to model interactions. Deo and Trivedi introduced CS-LSTM [4], an LSTM-based encoder-decoder model where a social pooling layer using convolutional connections, namely convolutional social pooling, is used to model vehicle interactions. Similarly, Messaoud et al. introduced a Multi-Head Attention (MHA) mechanism [5] to model distant traffic participants.

In recent developments, in addition to convolutional social pooling and attention mechanisms, Graph Neural Networks

(GNNs) have gained traction to create a scene graph and represent the neighboring participants as nodes. Mo et al. [6] employ Graph Attention Networks (GATs) [20] to model the neighboring vehicle interactions. The authors of Repulsion and Attraction Graph Attention (RA-GAT) [21] also use GATs to model the repulsive and attractive forces within a traffic scenario. Wu et al. [22] introduced Hierarchical Spatio-Temporal Attention (HSTA) for modeling spatio-temporal interactions and trajectory prediction using GATs, MHAs, along with LSTMs. Despite the widespread success of LSTM-based models, their limited memory capacity hinders their performance in capturing long-term dependencies. The introduction of exponential gating and augmented memory structures by the xLSTM architecture expands upon the conventional LSTM, enhancing the model's ability to capture long-range temporal dependencies.

B. Physics-Based Trajectory Prediction

Incorporating physical constraints leads to the prediction of physically feasible trajectories, which are often overlooked by data-driven deep learning approaches. The kinematic bicycle model describes the motion of a vehicle relying heavily on the vehicle dynamics to predict the trajectory in accordance with physical laws. Cui et al. [7] combine a deep learning-based method with the kinematic layer to explicitly encode vehicle kinematics to generate feasible motion of the traffic participants rather than relying on the deep learning models to learn the kinematic constraints from the data. This hybrid model proved to generate trajectories that are safe and feasible. The same methodology was followed by Neumeier et al. [23] and Wang et al. [24] to integrate the kinematic bicycle model into their network, enforcing physical consistency in the predicted trajectories, thus ensuring that the future paths follow realistic vehicular motion dynamics. Conventional LSTM architectures integrated with a kinematic layer might still suffer from limited memory capacity due to their scalar cell states. To overcome this, a kinematic layer is combined with an xLSTM architecture that provides enhanced representational capacity and rich memory structures.

III. xLSTM-BASED VEHICLE TRAJECTORY PREDICTION

This section formulates the problem of precise vehicle trajectory prediction and introduces the proposed xLSTM-based framework along with its components. Followed by this, the integration of the kinematic layer into the framework is presented to produce realistic and physically plausible future trajectories.

A. Preliminaries

Beck et al. introduced xLSTM [8] with two novel building blocks: sLSTM and mLSTM, to overcome the limitations of original LSTMs [3]. In our trajectory prediction framework, an sLSTM block is employed as the encoder. Exponential gating combined with normalization and stabilization is used to provide sLSTM the ability to revise storage decisions. In addition to this, sLSTM can have multiple heads that

enable memory mixing via recurrent connections R_x where $x \in \{i, f, o\}$ from the hidden state vector to memory cell input z and the gates i, f, o . This new way of memory mixing is possible within each head but not across heads. The forward pass of sLSTM is given by [8]:

$$\begin{aligned} \mathbf{c}_t &= \mathbf{f}_t \odot \mathbf{c}_{t-1} + \mathbf{i}_t \odot \mathbf{z}_t, \\ \mathbf{n}_t &= \mathbf{f}_t \odot \mathbf{n}_{t-1} + \mathbf{i}_t, \\ \mathbf{h}_t &= \mathbf{o}_t \odot \tilde{\mathbf{h}}_t, \quad \tilde{\mathbf{h}}_t = \mathbf{c}_t \odot \mathbf{n}_t^{-1}, \\ \mathbf{z}_t &= \varphi(\tilde{\mathbf{z}}_t), \quad \tilde{\mathbf{z}}_t = \mathbf{W}_z^\top \mathbf{x}_t + \mathbf{R}_z \mathbf{h}_{t-1} + \mathbf{b}_z, \\ \mathbf{i}_t &= \exp(\tilde{\mathbf{i}}_t), \quad \tilde{\mathbf{i}}_t = \mathbf{W}_i^\top \mathbf{x}_t + \mathbf{R}_i \mathbf{h}_{t-1} + \mathbf{b}_i, \\ \mathbf{f}_t &= \sigma(\tilde{\mathbf{f}}_t) \text{ or } \exp(\tilde{\mathbf{f}}_t), \quad \tilde{\mathbf{f}}_t = \mathbf{W}_f^\top \mathbf{x}_t + \mathbf{R}_f \mathbf{h}_{t-1} + \mathbf{b}_f, \\ \mathbf{o}_t &= \sigma(\tilde{\mathbf{o}}_t), \quad \tilde{\mathbf{o}}_t = \mathbf{W}_o^\top \mathbf{x}_t + \mathbf{R}_o \mathbf{h}_{t-1} + \mathbf{b}_o, \end{aligned} \quad (1)$$

where $\mathbf{c}_t, \mathbf{n}_t, \mathbf{h}_t \in \mathbb{R}^d$ represent the cell state, normalizer state, and hidden state, respectively, and \odot is element-wise multiplication. φ is the cell input activation function, typically \tanh , σ is sigmoid and \exp is exponential activation function. $\mathbf{W}_z, \mathbf{W}_i, \mathbf{W}_f, \mathbf{W}_o$ are the input weight matrices between inputs \mathbf{x}_t and cell input, input gate, forget gate, and output gate, respectively. $\mathbf{R}_z, \mathbf{R}_i, \mathbf{R}_f, \mathbf{R}_o$ correspond to the recurrent weights between hidden state \mathbf{h}_{t-1} and cell input, input gate, forget gate, and output gate, respectively. The corresponding bias terms are $\mathbf{b}_z, \mathbf{b}_i, \mathbf{b}_f, \mathbf{b}_o$. A detailed discussion of (1), as well as comparison to conventional LSTMs, can be found in [8].

B. Problem Definition

The aim is to predict the future trajectory of the target vehicle on a highway using historical trajectories of neighboring vehicles from time $t = 1$ to $t = t_{\text{obs}}$. The input to the model is the history of the target and its N surrounding vehicles in the same lane as the target vehicle and the lanes adjacent to the target vehicle lane. The input trajectory of a vehicle i is defined as $\mathbf{X}_i = [\mathbf{x}_i^1, \mathbf{x}_i^2, \dots, \mathbf{x}_i^{t_{\text{obs}}}]$ where $\mathbf{x}_i^t = [x_i^t, y_i^t, v_i^t, a_i^t]^\top$. Here, x_i^t and y_i^t denote the position coordinates of the vehicle i at time t , and v_i^t, a_i^t are the velocity and acceleration, respectively.

The position coordinates of all the vehicles are represented in a stationary frame of reference with the origin fixed at the target vehicle's position at time $t = 1$. The x -axis points towards the direction of motion on the highway, and the y -axis points downward, perpendicular to the x -axis.

The xLSTM-based model, X-TRAJ, outputs the predicted positions of the target vehicle for the next t_f time steps.

$$\mathbf{Y}_{\text{pred}} = [\mathbf{y}_{\text{pred}}^{t_{\text{obs}}+1}, \mathbf{y}_{\text{pred}}^{t_{\text{obs}}+2}, \dots, \mathbf{y}_{\text{pred}}^{t_{\text{obs}}+t_f}], \quad (2)$$

where $\mathbf{y}_{\text{pred}}^t = [x_{\text{pred}}^t, y_{\text{pred}}^t]^\top$ is the predicted position coordinates of the target vehicle at time t .

For the xLSTM-based kinematic model, the input of the model is defined in a similar way as $\mathbf{X}_i = [\mathbf{x}_i^1, \mathbf{x}_i^2, \dots, \mathbf{x}_i^{t_{\text{obs}}}]$, where instead of taking $[x_i^t, y_i^t, v_i^t, a_i^t]^\top$ as input features, it is

defined as $\mathbf{x}_i^t = [a_{x,i}^t, \dot{\psi}_i^t]^\top$, representing the vehicle's kinematic state using longitudinal acceleration (a_x) and yaw rate ($\dot{\psi}$). Similarly, the model predicts $\mathbf{y}_{\text{pred}}^t = [a_{x,\text{pred}}^t, \dot{\psi}_{\text{pred}}^t]^\top$ i.e., the longitudinal acceleration and yaw rate for the next time steps.

C. Overall Framework

In this section, the trajectory prediction framework is defined and illustrated in Fig. 1. The proposed model architecture features an encoder-decoder structure, where an sLSTM encoder block processes the sequential position of each vehicle in the traffic scenario to represent the temporal evolution of historical trajectories. To model social interactions, the encoded vectors are forwarded to GAT to extract the attention scores of the vehicles involved and create a context vector. The decoding layer predicts the future trajectory of the target vehicle using the extracted context and target vehicle encoding. Our architecture uses the strengths of social modeling, first introduced by Mo et al. [6], and differs in two significant aspects: an xLSTM encoder is employed to capture the long-term dependencies better, and a physics-based kinematics model is introduced to generate more plausible trajectories.

1) *Historical Encoder*: This layer encodes the trajectory of the neighboring vehicles as well as the target vehicle. A fixed set of $N = 8$ neighboring vehicles is considered, namely the preceding, following, left preceding, left alongside, left following, right preceding, right alongside, and right following vehicles. For every neighboring vehicle i , the state vector at time t , denoted as \mathbf{x}_i^t , is passed through a fully connected layer to create an embedding \mathbf{e}_i^t :

$$\mathbf{e}_i^t = \Psi(\mathbf{x}_i^t; \mathbf{W}_{\text{emb}}), \quad (3)$$

where $\Psi(\cdot)$ is implemented as a fully connected layer with a LeakyReLU activation, and \mathbf{W}_{emb} represents the learnable weights. xLSTM encoder captures the temporal dynamics by processing these embedding vectors sequentially.

$$\mathbf{h}_i^t = \text{xLSTM}(\mathbf{h}_i^{t-1}, \mathbf{e}_i^t; \mathbf{W}_{\text{enc}}), \quad (4)$$

where \mathbf{h}_i^t denotes the hidden state of the vehicle i at time t and \mathbf{W}_{enc} are the encoder weights. In the case of the encoder, an sLSTM block is employed.

2) *Modeling Vehicle Interactions*: The interaction among vehicles is modeled as a graph where each vehicle i in the scenario is represented as a node in a graph, with the central node being our target vehicle. The central node is indexed at 0 and all the neighboring vehicles are indexed at $1, \dots, N$.

$$\mathbf{E} = \{e^{0,j}\}_{j=1}^N, \quad (5)$$

where $e^{0,j}$ is a directed edge from node j to node 0 (the target vehicle node) which implies that node j is a neighbor of target node and node 0's behavior is impacted by node j 's behavior.

At each time t , node features are the xLSTM encoder states $\mathbf{h}_i^t \in \mathbb{R}^d$. A two-layer multi-head GAT model is used to predict the pairwise vehicular interactions within the traffic scenario. The hidden state \mathbf{h}_i^t is passed through two successive GAT [20] layers $\mathcal{G}_1(\cdot)$ and $\mathcal{G}_2(\cdot)$ that compute attention scores over

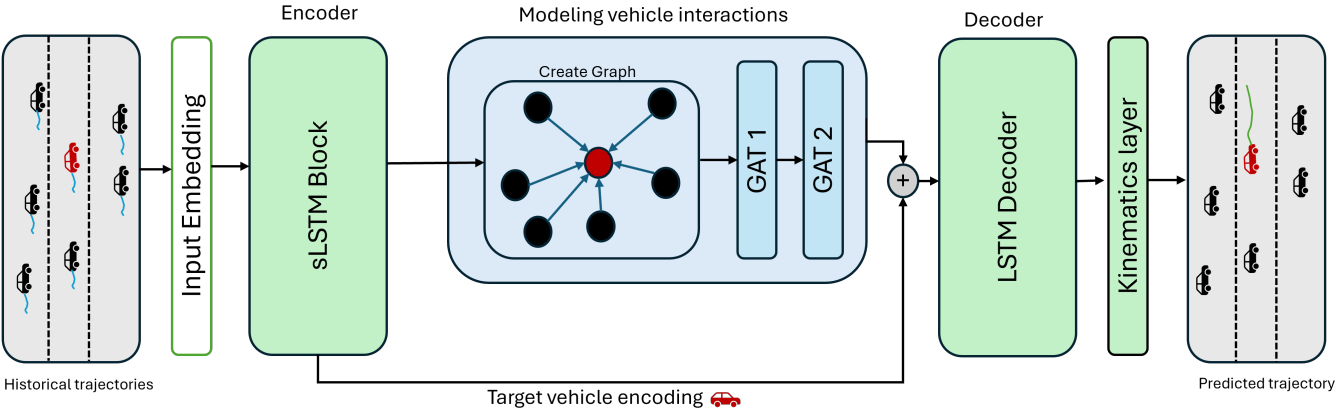


Fig. 1. **Proposed X-TRACK architecture:** The sLSTM block generates an encoded vector for all the vehicles in the traffic scenario. The GAT layers model the vehicle interactions between the target vehicle (shown in red) and the neighboring vehicles based on attention scores. The concatenation of the output from the GAT module and target vehicle encoding is passed through the decoder to predict future motion parameters. The Kinematic layer then transforms these motion parameters into position coordinates to provide the future trajectory of the target vehicle.

neighbors and aggregate their messages; outputs $\tilde{\mathbf{z}}_T^t$ of the target vehicle T are projected by a linear layer to produce an interaction feature \mathbf{g}_T^t .

$$\begin{aligned} \mathbf{z}_i^t &= \mathcal{G}_1(\mathbf{h}_i^t; \mathbf{W}_{\text{gat1}}), \\ \tilde{\mathbf{z}}_i^t &= \mathcal{G}_2(\mathbf{z}_i^t; \mathbf{W}_{\text{gat2}}), \\ \mathbf{g}_i^t &= \Phi(\tilde{\mathbf{z}}_i^t; \mathbf{W}_{\text{fc}}), \end{aligned} \quad (6)$$

where \mathbf{W}_{gat1} and \mathbf{W}_{gat2} are the learnable weights of GAT layers. $\Phi(\cdot)$ is a fully connected layer with LeakyReLU activation and \mathbf{W}_{fc} are the learned projection weights.

3) *Future Decoder:* LSTM decoder predicts the future trajectory of the target vehicle T using the concatenation of the target vehicle's encoding vector \mathbf{h}_T^t and interaction vector \mathbf{g}_T^t generated by the GAT module. The LSTM layer is followed by a fully connected layer that outputs the future position coordinates of the target vehicle for time steps $t = t_{\text{obs}} + 1, t_{\text{obs}} + 2, \dots, t_{\text{obs}} + t_f$:

$$\mathbf{y}_t^t = \Lambda\left(\text{LSTM}\left([\mathbf{h}_T^t; \mathbf{g}_T^t], \mathbf{h}_{\text{dec}}^{t-1}; \mathbf{W}_{\text{dec}}\right)\right), \quad (7)$$

where \mathbf{y}_t^t is the predicted position of the target vehicle at time t . The mapping function $\Lambda(\cdot)$ consists of a fully connected layer followed by LeakyReLU non-linearity. The decoder is parameterized by the learnable weights \mathbf{W}_{dec} , and the hidden state vector from the previous time step is $\mathbf{h}_{\text{dec}}^{t-1}$.

4) *Physics-based Kinematic Layer:* This module aims to predict the motion parameters, yaw rate $\dot{\psi}^t$ and longitudinal acceleration a_x^t of the vehicle instead of directly predicting the position coordinates, as described in III-C3. The encoder-decoder structure remains the same; however, the input to the physics-aware variant, X-TRACK, is $\mathbf{X}_i = [\mathbf{x}_i^1, \mathbf{x}_i^2, \dots, \mathbf{x}_i^{t_{\text{obs}}}]$, where $\mathbf{x}_i^t = [a_{x,i}^t, \dot{\psi}_i^t]^\top$.

To compute ground truth, numerical derivatives $\mathbf{a}_x = \frac{d^2 \mathbf{x}_{\text{pred}}}{dt^2}$ and $\dot{\psi} = \arctan\left(\frac{dy_{\text{pred}}}{dt}, \frac{dx_{\text{pred}}}{dt}\right)$ are calculated. From the predicted $\mathbf{Y}_{\text{pred}} = [\mathbf{y}_{\text{pred}}^{t_{\text{obs}}+1}, \mathbf{y}_{\text{pred}}^{t_{\text{obs}}+2}, \dots, \mathbf{y}_{\text{pred}}^{t_{\text{obs}}+t_f}]$, where $\mathbf{y}_{\text{pred}}^t = [a_{x,\text{pred}}^t, \dot{\psi}_{\text{pred}}^t]^\top$, the position $[x^t, y^t]^\top$, velocity

v^t and heading angle ψ^t of a vehicle at time step $t + \Delta t$ are computed as shown below [23], [25]:

$$\begin{aligned} x^{t+\Delta t} &= x^t + v^t c(\psi^t) \Delta t + \left(a_x^t c(\psi^t) - \dot{\psi}^t v^t s(\psi^t)\right) \frac{\Delta t^2}{2} \\ y^{t+\Delta t} &= y^t + v^t s(\psi^t) \Delta t + \left(a_x^t s(\psi^t) + \dot{\psi}^t v^t c(\psi^t)\right) \frac{\Delta t^2}{2} \\ v^{t+\Delta t} &= v^t + a_x^t \Delta t \\ \psi^{t+\Delta t} &= \psi^t + \dot{\psi}^t \Delta t, \end{aligned} \quad (8)$$

where $c(\psi^t) = \cos(\psi^t)$, $s(\psi^t) = \sin(\psi^t)$, ψ^t being the heading angle at time t and Δt is the time step size.

The predicted motion parameters are bounded by the physical limits $a_{x,\text{max}} = \pm 9 \text{ m/s}^2$ [26] and $\dot{\psi}_{\text{max}} = \pm 71.26 \text{ deg/s}$ [27] to ensure that the predicted trajectory is feasible to be executed by the target vehicle. The X-TRACK model does not rely on position coordinates to understand the vehicle dynamics; instead, it uses non-holonomic constraints of the vehicle to predict reliable future motion.

IV. DATASET, EXPERIMENTS AND EVALUATION

A. Datasets

To evaluate the performance of the trajectory prediction task of the proposed method, publicly available datasets, Highway Drone (highD) and Next Generation SIMulation (NGSIM), are used.

highD: The dataset has naturalistic vehicle trajectories captured using a drone at six different highway locations in Germany. It includes more than 110500 vehicles, 44500 driven kilometers, and 147 driven hours provided in 60 recordings with a sample rate of $f = 25 \text{ Hz}$. There is a large imbalance in scenarios where keep lane scenarios are more frequent than lane change scenarios [28]. To address this, traffic scenarios are extracted during the preprocessing step to ensure uniform distribution. Later, the extracted scenarios are split into subsets with 70 : 10 : 20 ratio: train, validation, and test with 9604, 1371, 2747 samples, respectively.

NGSIM: The dataset was recorded on US highways US-101, I-80 with a sample rate of $f = 10$ Hz. To capture different traffic conditions, three different 15 min time slots were chosen on both highways, making the total recording time 45 min. Similar to highD, NGSIM also has a huge imbalance of scenarios [21]. Therefore, the data is preprocessed in a similar way to extract an equal proportion of each scenario type. This, in turn, heavily reduces the total number of scenarios in the NGSIM dataset; however, training on a balanced dataset is crucial to avoid biasing the model towards lane-keeping scenarios, which constitute the majority class in both datasets [29]. The proportionate dataset is then split into train, validation, and test sets with 1634, 232, and 471 scenarios, respectively. Each extracted scenario is of 8s, with the first 3s representing the observed historical track and the next 5s as the future trajectory or the ground truth. In scenarios with insufficient surrounding context, such as when only a few surrounding vehicles are present, ghost vehicles are inserted while training X-TRAJ. These vehicles are provided with the same motion features as the target vehicle.

B. Training and Implementation Details

The model¹ is implemented using PyTorch [30] and GAT layers using PyTorch Geometric [31]. The encoder layer is implemented using a single-layer sLSTM block [8] with a 64-dimensional hidden state ($C = 64$) and the LSTM decoder with a 128-dimensional hidden state. The GAT layer [20] is configured with a concatenated four-head attention mechanism. The input features are transformed into a 32-dimensional embedding space before being processed by the encoder. The LeakyReLU activation function with a negative slope of 0.1 is used. A batch size of 32 is used during training, and optimization is carried out with the Adam [32] algorithm.

C. Evaluation Metrics

The following commonly used metrics are used to report and evaluate our model as compared to baselines:

Average Displacement Error (ADE): The mean Euclidean distance between the predicted and ground truth trajectories averaged across all time steps and all trajectories.

$$ADE = \frac{1}{N t_f} \sum_{n=1}^N \sum_{t=t_{obs}+1}^{t_{obs}+t_f} \sqrt{(x_{gt,n}^t - x_{pred,n}^t)^2 + (y_{gt,n}^t - y_{pred,n}^t)^2} \quad (9)$$

Final Displacement Error (FDE): The Euclidean distance between the predicted and ground truth final positions for each trajectory, averaged over all trajectories.

$$FDE = \frac{1}{N} \sum_{n=1}^N \sqrt{(x_{gt,n}^{t_{obs}+t_f} - x_{pred,n}^{t_{obs}+t_f})^2 + (y_{gt,n}^{t_{obs}+t_f} - y_{pred,n}^{t_{obs}+t_f})^2} \quad (10)$$

Root Mean Square Error (RMSE) at time t : The square root of

¹The code will be made publicly available upon acceptance to facilitate reproducibility.

the average of the squared differences between the predicted and corresponding ground truth positions for all N trajectories.

$$RMSE(t) = \sqrt{\frac{1}{N} \sum_{n=1}^N \left[(x_{gt,n}^t - x_{pred,n}^t)^2 + (y_{gt,n}^t - y_{pred,n}^t)^2 \right]} \quad (11)$$

D. Comparison with Baselines

For evaluation, the model's performance is compared against state-of-the-art methods. The models considered for comparison are:

- **Convolutional Social LSTM (CS-LSTM)** [4]: To model vehicle interaction, CS-LSTM uses convolution layers with social pooling and an LSTM-based encoder-decoder.
- **Graph and Recurrent Neural Network (Two Channel)** [6]: Utilizes GATs to model social interactions with a GRU encoder and LSTM decoder to predict the future path of the vehicle.
- **Multi-Head Attention LSTM (MHA-LSTM)** [5]: an LSTM-based encoder-decoder model that leverages both global and local attention mechanisms to capture social interactions between the target and its neighboring vehicles.
- **Repulsion and Attraction Graph Attention (RA-GAT)** [21]: Model vehicle and spaces as nodes in a graph and employ a dual graph attention mechanism to model repulsion from surrounding vehicles and attraction to the non-vehicle spaces.
- **Hierarchical Spatio-Temporal Attention (HSTA)** [22]: MHA is used to encode temporal correlations of interactions along with GAT to capture spatial interactions, followed by a state-gated fusion layer to integrate both spatial and temporal dependencies.
- **Graph Fourier Transformation Neural Network (GFTNNv2)** [28]: Vehicle interaction is transformed using Graph Fourier Transform (GFT) into a spectral scenario representation. This is fed to a neural network, and the prediction is converted to the spatio-temporal domain by applying the inverse GFT.
- **Graph-Based Spatial-Temporal Attentive Network (GSTAN)** [33]: To efficiently capture vehicle interactions, this model leverages attentive spatio-temporal modeling. The weighted distance GATs are integrated with dynamic attention assignment and modeled multi-headed social interaction patterns using MHA-based transformers.
- **X-TRAJ and X-TRACK:** The proposed model in this paper, where xlSTM is used to encode relationships with LSTM as a decoder and integrate it with the kinematic bicycle model to generate feasible trajectories. The two proposed models: one without the kinematic layer (X-TRAJ, see III-C3) and another with the kinematic layer (X-TRACK, see III-C4).

V. RESULTS AND DISCUSSION

Table I reports the ADE and FDE values for compared models on highD and NGSIM datasets, and Table II summarizes

TABLE I
ADE AND FDE METRICS FOR THE MODELS ON HIGHD AND NGSIM DATASETS

Architecture	highD		NGSIM	
	ADE [m]	FDE [m]@5s	ADE [m]	FDE [m]@5s
X-TRACK (Ours)	0.56	1.76	2.11	5.17
X-TRAJ (Ours)	1.14	2.65	<u>1.99</u>	4.99
CS-LSTM [4]	2.14	5.09	2.69	5.81
Two Channel [6]	2.08	4.84	2.89	6.26
MHA-LSTM [5]	1.97	4.72	2.54	5.47
RA-GAT [21]	1.99	4.83	2.70	5.88
HSTA [22]	1.99	4.60	2.54	5.80
GFTNNv2 [28]	<u>0.92</u>	<u>2.20</u>	2.26	<u>4.83</u>
GSTAN [33]	1.28	2.66	1.94	4.50

Note: The best results are in **bold**, and the second-best are underlined.

TABLE II
RMSE IN METERS OVER A 5-SECOND PREDICTION HORIZON FOR THE MODELS ON HIGHD AND NGSIM DATASETS

Dataset	Architecture	Prediction Horizon (s)				
		1	2	3	4	5
highD	X-TRACK (Ours)	0.10	0.31	0.71	1.31	2.16
	X-TRAJ (Ours)	0.48	1.01	1.58	2.20	3.17
	CS-LSTM [4]	0.76	1.77	3.08	4.66	6.52
	Two Channel [6]	0.81	1.70	2.94	4.41	6.14
	MHA-LSTM [5]	0.71	1.62	2.85	4.31	6.06
	RA-GAT [21]	0.67	1.58	2.79	4.29	6.06
	HSTA [22]	1.16	2.43	3.84	5.38	7.09
	GFTNNv2 [28]	<u>0.47</u>	<u>0.61</u>	<u>1.05</u>	<u>1.75</u>	<u>2.69</u>
	GSTAN [33]	0.51	1.02	1.60	2.23	3.09
NGSIM	X-TRACK (Ours)	0.68	1.78	3.25	4.80	6.67
	X-TRAJ (Ours)	<u>0.73</u>	1.65	<u>2.84</u>	<u>4.11</u>	6.44
	CS-LSTM [4]	1.17	2.24	3.84	5.64	7.66
	Two Channel [6]	1.23	2.50	4.17	6.04	8.15
	MHA-LSTM [5]	1.17	2.14	3.60	5.22	7.11
	RA-GAT [21]	1.24	2.24	3.80	5.54	7.65
	HSTA [22]	0.97	2.11	3.66	5.35	7.40
	GFTNNv2 [28]	0.99	1.98	3.26	4.67	<u>6.30</u>
	GSTAN [33]	0.89	<u>1.66</u>	2.74	4.00	5.90

Note: The best results are in **bold**, and the second-best are underlined.

the RMSE errors over the 5-second prediction horizon. All the models were implemented (in case the code was not available), trained, and evaluated on the balanced dataset resulting from the data preprocessing step as described in IV-A. The dataset is adjusted to accommodate the input required by the evaluated models. Both the models proposed in this paper, X-TRAJ and X-TRACK, achieve the best performance across all evaluation metrics in highD and performance comparable to state-of-the-art baselines in the case of NGSIM.

On highD, the integration of the kinematic layer to our xLSTM-based vehicle trajectory prediction framework yields substantial improvements: 51% in ADE and 34% in FDE. For RMSE, the X-TRACK model improves by 79% at the 1-second prediction and by 32% at the 5-second prediction. This performance enhancement indicates that the non-holonomic constraints introduced by the kinematic layer enforce physically consistent motion and prevent implausible

trajectory drift. Fig. 2 shows the predicted trajectories of X-TRAJ and X-TRACK on the highD dataset, showing that X-TRACK exhibits closer alignment with the ground-truth trajectory. Compared to MHA-LSTM [5], the proposed X-TRACK achieves 86% better performance at the 1-second prediction horizon and 64% at the 5-second prediction horizon. In comparison to GFTNNv2 [28], X-TRACK shows 78.7% and 19.7% improvement at 1-second and 5-second prediction, respectively. Additionally, due to the missing physical constraints, X-TRAJ performs 2.13% worse than GFTNNv2 at 1-second prediction and 17.84% worse than GFTNNv2 at 5-second prediction on the highD dataset.

In the case of NGSIM, X-TRAJ achieves better performance, with 6.03% improvement in ADE and 3.61% improvement in FDE, compared to X-TRACK. The second-best performance is achieved by X-TRAJ preceded by GSTAN [33] with 2.58% and 10.89% improvement in ADE and

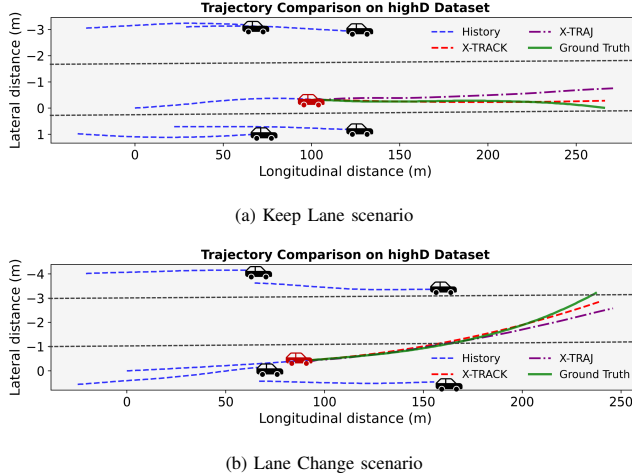


Fig. 2. Comparison of predicted trajectories on the highD dataset using X-TRAJ and X-TRACK in case of (a) Keep lane (b) Lane change.

FDE, respectively. In terms of RMSE, the lowest RMSE at 1-second is achieved by X-TRACK, and at 5-second is achieved by GSTAN. In comparison to MHA-LSTM [5], X-TRACK performs 42% and 6% better at RMSE 1-second and 5-second prediction, respectively. X-TRACK shows 23.6% better performance than GSTAN [28] at 1-second RMSE and 13.05% worse performance at 5-second RMSE.

In comparison to the highD dataset, the evaluated models have higher errors in terms of ADE, FDE, and RMSE on the NGSIM dataset. Additionally, the performance gain in highD is more pronounced compared to NGSIM. One possible reason could be the limited number of scenarios that were extracted to create a proportionate dataset. As the original dataset exhibits a substantial imbalance in scenarios, it is not reasonable to train on the entire dataset, because the model would primarily learn the dominant keep lane behavior, leading to biased predictions. Therefore, after preprocessing, the number of scenarios was reduced to 2337 scenarios, which is approximately 6 times less than the number of scenarios in highD. This small dataset size could potentially lead to overfitting and might affect the model's ability to generalize to unseen data. Another possible reason pointed out by Coifman et al. [34] could be the annotation inaccuracies, which result in complex and physically unrealistic behaviors in the dataset. In comparison to NGSIM, highD consists of well-annotated highway scenarios with smoother trajectories. This indicates that these inaccuracies could be one of the reasons why adding the kinematic layer to X-TRAJ in the case of NGSIM does not show a performance gain. Overall, X-TRACK significantly and consistently outperforms state-of-the-art models on the highD dataset and is among the top-performing models on NGSIM.

A. Effects of using different xLSTM blocks in X-TRACK

Table III shows the ADE and FDE metrics of the xLSTM-based kinematic model, X-TRACK, using either LSTM, sLSTM, or mLSTM for the encoder-decoder combination. It was observed that using sLSTM as an encoder and LSTM

as a decoder produces the lowest error as compared to other configurations. The worst performance is observed when sLSTM is used as an encoder and mLSTM as a decoder, and all the other configuration shows similar performance. The sLSTM encoder in combination with the LSTM decoder achieves 10.77% and 6.5% performance improvement in ADE and FDE, respectively, than the conventional LSTM encoder-decoder architecture with an integrated physics-based kinematic model.

TABLE III
ADE AND FDE METRICS TO COMPARE DIFFERENT ENCODER-DECODER COMBINATIONS IN X-TRACK

Encoder	Decoder	ADE [m]	FDE [m]@5s
LSTM	sLSTM	0.63	1.78
LSTM	mLSTM	0.62	1.76
LSTM	LSTM	0.65	1.85
sLSTM	sLSTM	0.64	1.83
sLSTM	mLSTM	0.72	1.97
sLSTM	LSTM	0.56	1.76

VI. CONCLUSION

This paper introduced a novel xLSTM-based vehicle trajectory prediction framework, X-TRAJ, and its physics-augmented extension, X-TRACK, for vehicle trajectory prediction on highways. The experimental results confirm that replacing xLSTM with a conventional LSTM in the X-TRACK leads to a noticeable drop in performance. The xLSTM-based model when integrated with the kinematic layer, X-TRACK, achieves up to 10.77% improvement in ADE and 6.5% in FDE metrics, underscoring its ability to capture long-term temporal dependencies more effectively.

By integrating a physics-based kinematic module to X-TRAJ, the proposed X-TRACK achieves an improvement of up to 79% at a 1-second prediction horizon and about 32% at a 5-second prediction horizon on the highD dataset, demonstrating that the use of non-holonomic vehicle constraints leads to smoother and physically consistent predictions. The kinematic module enables more accurate prediction of trajectories as the physical laws of vehicle dynamics are known and not required to be inferred from the data in the case of deep learning-based models. Compared to state-of-the-art baselines, X-TRACK achieves performance improvement by 79% at the 1-second prediction and 20% at the 5-second prediction in the case of highD, compared to GFTNNv2 [28], the second-best approach. The evaluation on the NGSIM dataset indicates that X-TRACK is among the state-of-the-art models, though with the reduced dataset size in NGSIM, the results are less statistically significant as compared to the highD dataset.

These findings suggest that physics-based priors, when combined with data-driven sequence models, bridge the gap between predictive accuracy and physical consistency, which is essential in autonomous driving systems. Potential extensions include integration of additional information, such as richer road structure and map information, into our model to improve

scenario representation. Furthermore, the proposed xLSTM architecture could also be extended to urban driving datasets in order to evaluate its performance under more diverse and complex traffic environments.

ACKNOWLEDGMENT

This research was supported by Technische Hochschule Augsburg and the Hightech Agenda Bavaria, funded by the Free State of Bavaria, Germany. The authors would like to thank their colleagues at Data Science und Autonome Systeme Technologietransferzentrum (TTZ) Landsberg for their insightful discussions and support.

REFERENCES

- [1] M. Bahari, H. Caesar, N. Navab, and T. F. C. de Campos, “Vehicle trajectory prediction works, but not everywhere,” in *Proceedings of the IEEE/CVF Conference on Computer Vision and Pattern Recognition (CVPR)*, (New Orleans, LA, USA), pp. 17102–17112, 2022.
- [2] V. Bharilya and N. Kumar, “Machine learning for autonomous vehicle’s trajectory prediction: A comprehensive survey, challenges, and future research directions,” *arXiv preprint arXiv:2307.07527*, 2023.
- [3] S. Hochreiter and J. Schmidhuber, “Long short-term memory,” *Neural Computation*, vol. 9, no. 8, pp. 1735–1780, 1997.
- [4] N. Deo and M. M. Trivedi, “Convolutional social pooling for vehicle trajectory prediction,” in *Proceedings of the IEEE Conference on Computer Vision and Pattern Recognition (CVPR)*, pp. 1549–15498, 2018.
- [5] K. Messaoud, I. Yahiaoui, A. Verroust-Blondet, and F. Nashashibi, “Attention based vehicle trajectory prediction,” *IEEE Transactions on Intelligent Vehicles*, pp. 175–185, 2021.
- [6] X. Mo, Y. Xing, and C. Lv, “Graph and recurrent neural network-based vehicle trajectory prediction for highway driving,” in *2021 IEEE International Intelligent Transportation Systems Conference (ITSC)*, pp. 1934–1939, IEEE, 2021.
- [7] H. Cui *et al.*, “Deep kinematic models for kinematically feasible vehicle trajectory predictions,” in *Proceedings of the IEEE International Conference on Robotics and Automation (ICRA)*, (Paris, France), pp. 10563–10569, 2020.
- [8] M. Beck, K. Pöppel, M. Spanring, A. Auer, O. Prudnikova, M. Kopp, G. Klambauer, J. Brandstetter, and S. Hochreiter, “xlstm: Extended long short-term memory,” *Advances in Neural Information Processing Systems*, vol. 37, pp. 107547–107603, 2024.
- [9] G. Gil, P. Duhamel-Sebline, and A. Mccarren, “An evaluation of deep learning models for stock market trend prediction,” *arXiv preprint arXiv:2408.12408*, 2024.
- [10] M. Alharthi and A. Mahmood, “xlstmtime: Long-term time series forecasting with xlstm,” *AI*, vol. 5, no. 3, pp. 1482–1495, 2024.
- [11] M. Kraus, F. Divo, D. S. Dhami, and K. Kersting, “xlstm-mixer: Multivariate time series forecasting by mixing via scalar memories,” *arXiv preprint arXiv:2410.16928*, 2024.
- [12] A. Auer *et al.*, “Tirex: Zero-shot forecasting across long and short horizons with enhanced in-context learning,” *arXiv preprint arXiv:2505.23719*, 2025.
- [13] Y. Huang, J. Du, Z. Yang, Z. Zhou, L. Zhang, and H. Chen, “A survey on trajectory-prediction methods for autonomous driving,” *IEEE Transactions on Intelligent Vehicles*, vol. 7, no. 3, pp. 652–674, 2022.
- [14] T. Elter, T. Dirndorfer, M. Botsch, and W. Utschick, “Interaction-aware prediction of occupancy regions based on a pomdp framework,” in *Proceedings of the IEEE International Conference on Intelligent Transportation Systems (ITSC)*, pp. 980–987, 2022.
- [15] S. Ulbrich and M. Maurer, “Probabilistic online pomdp decision making for lane changes in fully automated driving,” in *Proceedings of the 16th IEEE International Conference on Intelligent Transportation Systems (ITSC)*, pp. 2063–2067, 2013.
- [16] C.-E. Framing, F.-J. Heßeler, and D. Abel, “Infrastructure-based vehicle maneuver estimation with intersection-specific models,” in *Proceedings of the 26th Mediterranean Conference on Control and Automation (MED)*, pp. 253–258, 2018.
- [17] S. Lefèvre, D. Vasquez, and C. Laugier, “A survey on motion prediction and risk assessment for intelligent vehicles,” *Robomech Journal*, vol. 1, 2014.
- [18] H. Yin, Y. Wen, and J. Li, “A survey of vehicle trajectory prediction based on deep learning,” in *Proceedings of the 3rd International Conference on Neural Networks, Information and Communication Engineering (NNICE)*, pp. 140–144, Feb. 2023.
- [19] A. Alahi, K. Goel, V. Ramanathan, A. Robicquet, L. Fei-Fei, and S. Savarese, “Social lstm: Human trajectory prediction in crowded spaces,” in *Proceedings of the IEEE Conference on Computer Vision and Pattern Recognition (CVPR)*, pp. 961–971, 2016.
- [20] P. Velicković, G. Cucurull, A. Casanova, A. Romero, P. Liò, and Y. Bengio, “Graph attention networks,” *arXiv preprint arXiv:1710.10903*, 2017.
- [21] Z. Ding, Z. Yao, and H. Zhao, “Ra-gat: Repulsion and attraction graph attention for trajectory prediction,” in *Proceedings of the IEEE International Conference on Intelligent Transportation Systems (ITSC)*, pp. 734–741, 2021.
- [22] Y. Wu, G. Chen, Z. Li, L. Zhang, L. Xiong, Z. Liu, and A. Knoll, “Hsta: A hierarchical spatio-temporal attention model for trajectory prediction,” *IEEE Transactions on Intelligent Transportation Systems*, vol. 70, pp. 11295–11307, 2021.
- [23] M. Neumeier, S. Dorn, M. Botsch, and W. Utschick, “Reliable trajectory prediction and uncertainty quantification with conditioned diffusion models,” in *Proceedings of the IEEE/CVF Conference on Computer Vision and Pattern Recognition (CVPR) Workshops*, pp. 3461–3470, June 2024.
- [24] C. Wang, H. Liao, Z. Li, and C. Xu, “Wake: Towards robust and physically feasible trajectory prediction for autonomous vehicles with wavelet and kinematics synergy,” *IEEE Transactions on Pattern Analysis and Machine Intelligence*, vol. 47, pp. 3126–3140, Apr. 2025.
- [25] M. Botsch and W. Utschick, *Fahrzeugsicherheit und automatisiertes Fahren: Methoden der Signalverarbeitung und des maschinellen Lernens*. München: Hanser, 2020.
- [26] N. M. Yusof, J. Karjanto, J. Terken, F. Delbressine, M. Z. Hassan, and M. Rauterberg, “The exploration of autonomous vehicle driving styles: Preferred longitudinal, lateral, and vertical accelerations,” in *Proceedings of the 8th International Conference on Automotive User Interfaces and Interactive Vehicular Applications*, pp. 245–252, 2016.
- [27] J. Kontos, B. Kránicz, and Á. Vathy-Fogarassy, “Prediction for future yaw rate values of vehicles using long short-term memory network,” *Sensors*, vol. 23, no. 12, 2023.
- [28] M. Neumeier, S. Dorn, M. Botsch, and W. Utschick, “Prediction and interpretation of vehicle trajectories in the graph spectral domain,” 2023.
- [29] M. Neumeier, A. Tollkühn, M. Botsch, and W. Utschick, “A multidimensional graph fourier transformation neural network for vehicle trajectory prediction,” in *Proceedings of the 2022 IEEE 25th International Conference on Intelligent Transportation Systems (ITSC)*, (Macau, China), pp. 687–694, 2022.
- [30] A. Paszke, S. Gross, S. Chintala, G. Chanan, E. Yang, Z. DeVito, Z. Lin, A. Desmaison, L. Antiga, and T. K., “Automatic differentiation in pytorch,” in *Proceedings of the NIPS Autodiff Workshop: The Future of Gradient-Based Machine Learning Software and Techniques*, December 2017.
- [31] M. Fey and J. E. Lenssen, “Fast graph representation learning with PyTorch Geometric,” in *ICLR Workshop on Representation Learning on Graphs and Manifolds*, 2019.
- [32] D. P. Kingma and J. Ba, “Adam: A method for stochastic optimization,” in *Proceedings of the 3rd International Conference on Learning Representations (ICLR)*, May 2015.
- [33] D. E. Benrachou, S. Glaser, M. Elhenawy, and A. Rakotonirainy, “Graph-based spatial-temporal attentive network for vehicle trajectory prediction in automated driving,” *IEEE Transactions on Intelligent Transportation Systems*, 2025.
- [34] B. Coifman and L. Li, “A critical evaluation of the next generation simulation (ngsim) vehicle trajectory dataset,” *Transportation Research Part B: Methodological*, vol. 105, pp. 362–377, 2017.